APL Materials

Synthesis of $Ag_9(SiO_4)_2NO_3$ through a reactive flux method and its visible-light photocatalytic performances

Cite as: APL Mater. **3**, 104413 (2015); https://doi.org/10.1063/1.4928595
Submitted: 22 June 2015 • Accepted: 04 August 2015 • Published Online: 12 August 2015

Xianglin Zhu, Zeyan Wang, Baibiao Huang, et al.

Synthesis of $Ag_9(SiO_4)_2NO_3$ through a reactive flux method and its visible-light photocatalytic performances

Xianglin Zhu,[1] Zeyan Wang,[1,a] Baibiao Huang,[1,a] Wei Wei,[2] Ying Dai,[2] Xiaoyang Zhang,[1] and Xiaoyan Qin[1]
[1]*State Key Laboratory of Crystal Materials, Jinan 250100, People's Republic of China*
[2]*School of Physics, Shandong University, Jinan 250100, People's Republic of China*

(Received 22 June 2015; accepted 4 August 2015; published online 12 August 2015)

$Ag_9(SiO_4)_2NO_3$ was prepared by a reactive flux method. The structures, morphologies, and light absorption properties were investigated. Owing to the polar crystal structure, an internal electric field can be formed inside the material, which can facilitate the photogenerated charge separation during the photocatalytic process. Based on both the wide light absorption spectra and high charge separation efficiency originated from the polarized internal electric field, $Ag_9(SiO_4)_2NO_3$ exhibit higher efficiency over Ag_3PO_4 during the degradation of organic dyes under visible light irradiation, which is expected to be a potential material for solar energy harvest and conversion. [http://dx.doi.org/10.1063/1.4928595]

Photocatalysis has attracted increasing interests because of its potential applications to solve energy crisis and environmental pollutions by directly utilizing the natural solar energy. Great efforts have been made and various photocatalysts have been explored in the past forty years.[1–8] However, the photocatalytic efficiency is still greatly limited by the poor response to visible light and the low separation efficiency of photogenerated charge carriers. Therefore, the exploration of new photocatalysts with enhanced efficiencies has emerged as an urgent and challenging task in the field of photocatalysis.

Among the various photocatalysts, Ag-based photocatalyst is one of the most attractive candidates with excellent visible light absorptions and high photocatalytic activities. Due to the unique d^{10} electronic configurations of Ag^+ ions, they can take part in the composition and hybridization of the energy band in almost all the Ag-based compounds, which is beneficial to adjust the bandgap and light absorption properties of materials.[9–13] Additionally, part of the Ag^+ ions can be easily reduced into Ag nanoparticles under light irradiation, which can intensively increase the visible light absorption due to the localized surface plasmon resonance effects (LSPRs) of Ag nanoparticles and enhance the photocatalytic performances.[14] Up to now, various Ag-based photocatalysts have been reported, such as Ag@AgX (X=Cl, Br, I), Ag_3PO_4, Ag_2CO_3, Ag_3AsO_4,[15–20] and their exceptional visible light absorption, and excellent photocatalytic properties have been extensively investigated and demonstrated.

In order to further improve the photogenerated charge separation efficiency, many strategies have also been developed, e.g., doping, heterostructures, and modification with noble metal nanoparticles Different from these traditional strategies, recently, our investigations on polar photocatalysts, e.g., $BiOIO_3$, $Ag_6Si_2O_7$, $Bi_2O_2[BO_2(OH)]$, revealed that internal electric fields originated from the special crystal structures of polar materials could be another possible method to further facilitate the photogenerated charge separation.[21–23] Due to the existence of polarized construction units, such as IO_3, $BO_2(OH)$, or distorted SiO_4 tetrahedra, inside these polar photocatalysts, a strong electric field could be established all through the interior of the materials, which could drive the photogenerated

[a]Authors to whom correspondence should be addressed. Electronic addresses: wangzeyan@sdu.edu.cn and bbhuang@sdu.edu.cn

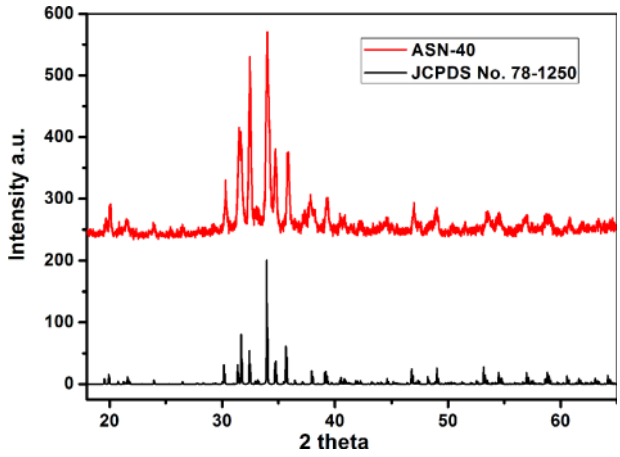

FIG. 1. XRD patterns of as-prepared sample $Ag_9(SiO_4)_2NO_3$.

electrons and holes to move oppositely and separate. Combining the unique photon energy harvesting properties of Ag-based compounds and the efficient charge separation of polar materials, Ag-based compounds with polar crystal structures could be potential candidates for high reactive photocatalysts with both strong visible light absorption and high electron-hole separation efficiencies.

$Ag_9(SiO_4)_2NO_3$ has a triclinic crystal structure constructed by separated single SiO_4 tetrahedra and NO_3 polyhedra coordinated with Ag ions. It has been reported that $Ag_9(SiO_4)_2NO_3$ has a narrow band gap of 1.95 eV with a strong absorption in visible light region due to the d^{10}-d^{10} interactions of the short Ag—Ag bonds, which make it a reactive photocatalyst with strong absorptions in visible light region.[24] However, the photocatalytic oxidation mechanism and the charge separation processes are still remain unclear. Herein, we reported the synthesis of $Ag_9(SiO_4)_2NO_3$ by a facile and simple flux method. The crystal structures, morphologies, and photocatalytic properties have been investigated. Based on the analysis about polar crystal structure of $Ag_9(SiO_4)_2NO_3$, a mechanism was proposed to explain the charge separation process. And the high photocatalytic activity of $Ag_9(SiO_4)_2NO_3$ can be ascribed to both the intensive visible light absorption and efficient charge separation originated from the internal electric field generated by the non-centrosymmetric triclinic polar crystal structure.

The XRD pattern of as-prepared sample was shown in Fig. 1. From this figure, we can find all the peaks can be indexed to the triclinic $Ag_9(SiO_4)_2NO_3$ (JCPDS No. 78-1250) without the appearance of any other impurities. The morphologies of as-prepared samples were characterized by scanning electron microscopy (SEM) as shown in Fig. 2. The as-prepared sample exhibits flower-like morphology comprised of nanosheets with irregular shapes (see Fig. 2(a)). For a closer observation, the sheet-like building blocks with smooth surfaces are of about 100-200 nm in width, 400-700 nm in length, and

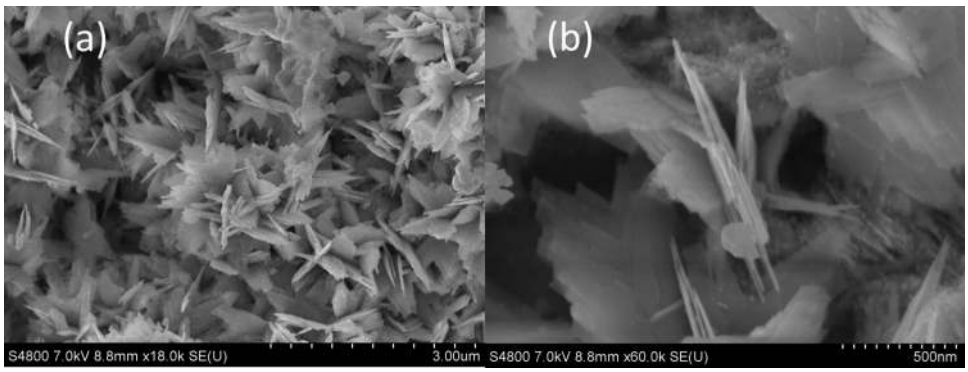

FIG. 2. SEM images of $Ag_9(SiO_4)_2NO_3$.

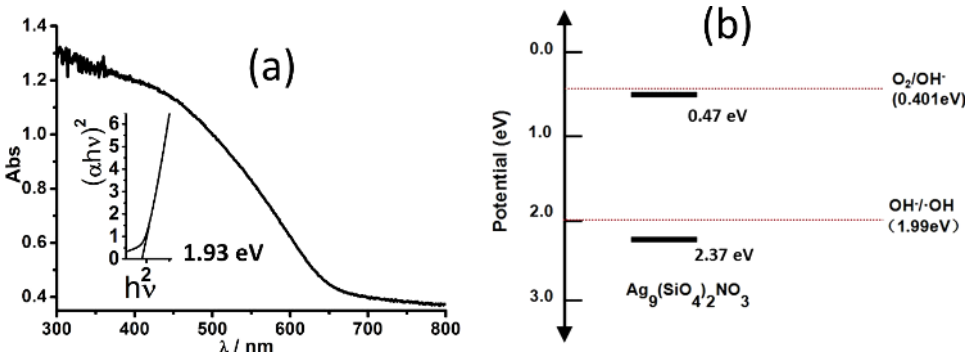

FIG. 3. (a) Diffused reflectance spectra and (b) the band-edge potentials of $Ag_9(SiO_4)_2NO_3$. The inset of (a) is the $(\alpha h\nu)^2$ versus $h\nu$ plot.

with thickness of about 20-50 nm (see Fig. 2(b)). Some small nanoparticles can be observed on the surface of the nanosheets, which could be probably silver nanoparticles formed by the reduction of Ag^+ in $Ag_9(SiO_4)_2NO_3$ under the irradiation of high energy electron beam during the SEM characterization, which is commonly observed in Ag containing compounds. The crystallite size of as-prepared $Ag_9(SiO_4)_2NO_3$ is estimated to be 22.26 nm calculated following Scherrer formula, which is quite close to the measured thickness of $Ag_9(SiO_4)_2NO_3$.

The reddish brown $Ag_9(SiO_4)_2NO_3$ powder is expected to be able to harvest visible light photon energies. As shown in the diffused reflectance spectra in Fig. 3, $Ag_9(SiO_4)_2NO_3$ exhibit a strong light absorption in visible-light region. And the band gap of as-prepared $Ag_9(SiO_4)_2NO_3$ is estimated to be 1.93 eV according to the $(\alpha h\nu)^2$ versus $h\nu$ plot shown in the inset of Fig. 3(a). Conduction band (CB) and valence band (VB) positions of $Ag_9(SiO_4)_2NO_3$ were also calculated following the empirical equation: $E_{VB} = \chi - E^e + 0.5E_g$. Details about the CB and VB calculations have been provided in the supplementary material.[25] And the estimated CB and VB band edges of $Ag_9(SiO_4)_2NO_3$ are 0.47 and 2.37 eV *vs* NHE (normal hydrogen electrode) as shown in Fig. 3(b), respectively, which indicate it can be used as oxidative photocatalyst.

In order to investigate the photocatalytic activity, $Ag_9(SiO_4)_2NO_3$ was evaluated by the photodegradation of organic dyes and O_2 production under visible light irradiation ($\lambda > 420$ nm). For comparison, Ag_3PO_4, known as an efficient visible light driven photocatalyst, was chosen as a reference. As shown in Fig. 4(a), the RhB dye solution can be almost completely bleached by $Ag_9(SiO_4)_2NO_3$ in 12 min (97%), whilst only 53% of RhB dye can be degraded within the same period by Ag_3PO_4. Similar results were also observed during the degradation of MB (Methylene blue) and MO (Methyl orange) dyes as shown in Fig. S1 of the supplementary material.[25] To verify the degradation of RhB dye molecules during the photocatalytic process, the total organic carbon (TOC) and inorganic carbon (IC) of RhB solution was measured over $Ag_9(SiO_4)_2NO_3$. As shown in Fig. 4(b), the TOC decreased from 15.52 ppm to 9.625 ppm, whilst the IC increased from 0.165 ppm to 7.61 ppm, which indicate the organic RhB dye molecules have been degraded into inorganic CO_2 during the photocatalytic process. Although the color of the RhB aqueous solution has been bleached, there is still some organic species in the solution according to the TOC measurement. This could be due to the intermediate products formed during the degradation of RhB dye molecules, which can be completely degraded by prolonging the photocatalytic reaction time.

The major reactive species of $Ag_9(SiO_4)_2NO_3$ during the photocatalytic degradation of RhB were determined by radical-trapping experiments by employing Na_2EDTA (a hole scavenger), $AgNO_3$ (an electron scavenger), and tert-butanol (an ·OH radical scavenger) under identical conditions. As shown in Fig. 4(c), the degradation rates slightly changes in presence of $AgNO_3$ and tert-butanol, suggesting the electrons and ·OH radicals are not the main reactive species during the photodegradation of RhB dye molecules. However, in presence of Na_2EDTA, the photocatalytic activity of $Ag_9(SiO_4)_2NO_3$ completely disappeared, indicating the photogenerated holes are the major reactive species during RhB degradation.

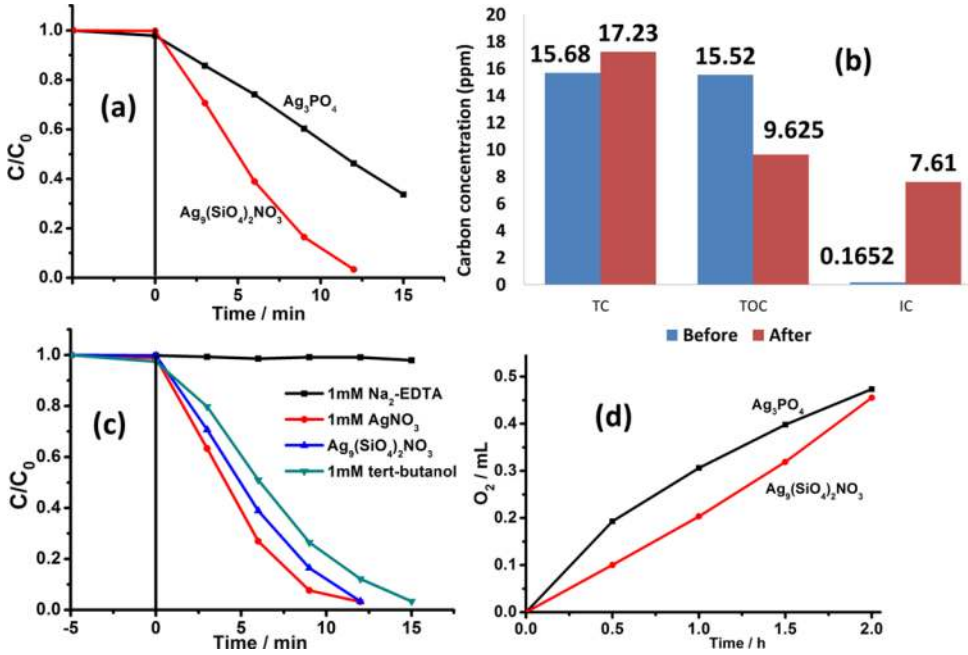

FIG. 4. Photodegradation of (a) RhB dye solutions over $Ag_9(SiO_4)_2NO_3$ and Ag_3PO_4, (b) the TOC and IC change during the photocatalytic experiments, (c) photodegradation of RhB in presence of Na_2EDTA, $AgNO_3$, and tert-butanol, (d) photocatalytic O_2 production from water under visible light irradiation ($\lambda > 420$ nm).

During the photocatalytic O_2-production experiments as shown in Fig. 4(d), $Ag_9(SiO_4)_2NO_3$ exhibit similar photocatalytic activity under visible light irradiation with Ag_3PO_4, which is regarded as one of the most reactive photocatalyst for O_2 evolution. Similar as the other Ag containing photocatalysts, the stability of $Ag_9(SiO_4)_2NO_3$ is relatively poor. As shown in the recycled photocatalytic experiments in Fig. S4 of the supplementary material,[25] 97% of RhB dye can be degraded in 12 min for the first run, but only 54% can be degraded in the same period for the second run. And the color of the samples turns from reddish brown to black, which could be ascribed to the formation of Ag nanoparticles formed by the photoreduction of Ag^+ originated from the partly dissolution of $Ag_9(SiO_4)_2NO_3$ in water and blocked the light absorption. This assumption can be later approved by that the color of $Ag_9(SiO_4)_2NO_3$ did not change in air without any protections even after one month, indicating Ag nanoparticles are formed by the reduction of Ag^+ ions dissolved in water. Further investigations on the stability of the samples are also needed.

The good photocatalytic performance of as prepared $Ag_9(SiO_4)_2NO_3$ could be attributed to its special morphology and smaller band gap comparing to Ag_3PO_4. The band gap of $Ag_9(SiO_4)_2NO_3$ is 1.93 eV, which is much smaller than that of Ag_3PO_4 (about 2.4 eV); thus it can absorb more photon energies and generate more electron-hole pairs. The BET surface area of $Ag_9(SiO_4)_2NO_3$ is 34.83 m^2/g, which is much larger than that of Ag_3PO_4 (4.41 m^2/g). However, further investigations indicate the surface areas of $Ag_9(SiO_4)_2NO_3$ could have little effect on its photocatalytic performances. As shown in Fig. S3 of the supplementary material,[25] $Ag_9(SiO_4)_2NO_3$ samples with different BET surface areas prepared with different reaction times exhibit similar photocatalytic activity, which indicates the contribution of the larger BET surface area of $Ag_9(SiO_4)_2NO_3$ could be excluded. Another factor that can contribute to the higher photocatalytic activity could be attributed to the polar crystal structure of $Ag_9(SiO_4)_2NO_3$, which can generate an internal electric field inside the material and facilitate the photogenerated charge separation. $Ag_9(SiO_4)_2NO_3$ has an asymmetric polar crystal structure belongs to the space group of P1 as shown in Fig. 5. However, its crystal structure is centrosymmetric regardless of the existence of NO_3^- groups in the material, which indicates the polarization inside the material is originated from NO_3^- groups in $Ag_9(SiO_4)_2NO_3$. Based on the bond-valence model, the dipole moment of NO_3^- in one crystal cell is calculated to be

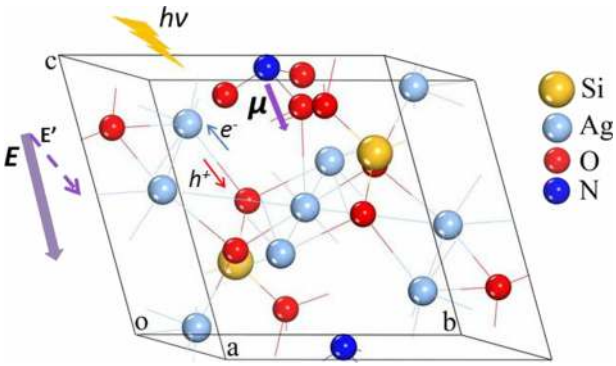

FIG. 5. The crystal structure and possible photocatalytic mechanism schematic diagram of $Ag_9(SiO_4)_2NO_3$. ***E*** is the internal electric field caused by polar crystal structure, and ***E′*** is the part along direction of one Ag—O bond.

about 159 D (see the supplementary material[25]), thus can generate an internal electric field along the direction as shown in Fig. 5. This assumption was soon verified by exciton lifetime measurements. As shown in Fig. S5,[25] the fluorescence lifetime of $Ag_9(SiO_4)_2NO_3$ is 2.6335 ns, which is longer than that of Ag_3PO_4 (1.8390 ns), indicates the charge separation efficiency in $Ag_9(SiO_4)_2NO_3$ is higher.

Based on the above results and discussions, a possible photocatalytic mechanism was proposed as illustrated in Fig. 5. As the CB and VB of $Ag_9(SiO_4)_2NO_3$ are mainly consisted of O and Ag atoms, respectively, according to the calculations (Fig. S6 of the supplementary material[25]), then the photon energy is absorbed by $Ag_9(SiO_4)_2NO_3$ and electrons from the VB are transferred to the CB, which can be described as electron transfer from O atoms to coordinated Ag atoms in the material. The existence of NO_3^- groups inside the material can generate internal electric fields, and its direction is accordant with the directions that electrons and holes move, which, therefore, can provide an additional driven force to facilitate the charge separation and result in enhanced photocatalytic activities.

In summary, we synthesized $Ag_9(SiO_4)_2NO_3$ through a simple flux method. The structures and morphologies were characterized by XRD and SEM, respectively. The as prepared $Ag_9(SiO_4)_2NO_3$ nanoflowers are constructed by some small nanosheets with thickness of about 20 nm. The band gap of $Ag_9(SiO_4)_2NO_3$ is 1.93 eV, which can absorb visible light up to about 650 nm. Additionally, due to its polar crystal structure, an internal electric field can be formed inside the materials, which can effectively improve the photogenerated charge separation. Owing to the wide visible light absorption and high charge separation efficiency, $Ag_9(SiO_4)_2NO_3$ exhibit high photocatalytic activity during the degradation of organic dyes and O_2 production under visible light irradiation comparing to Ag_3PO_4, which make it an ideal material for solar energy absorption and utilization.

This work was financially supported by a research grant from the National Basic Research Program of China (the 973 Program, Grant No. 2013CB632401), National Natural Science Foundation of China (Grant Nos. 21333006, 11374190, and 51321091), Shandong Provincial Natural Science Foundation (Grant No. ZR2014BM024), and Young Scholars Program of Shandong University (YSPSDU, Grant No. 2015WLJH35).

[1] A. Fujishima and K. Honda, Nature **238**, 37 (1972).
[2] Y. Peng, L. Shang, T. Bian, Y. F. Zhao, C. Zhou, H. J. Yu, L. Z. Wu, C.-H. Tung, and T. R. Zhang, Chem. Commun. **51**, 4677–4680 (2015).
[3] L. K. Pan, X. J. Liu, Z. Sun, and C. Q. Sun, J. Mater. Chem. A **1**, 8299–8326 (2013).
[4] Q. Wan, T. H. Wang, and J. C. Zhao, Appl. Phys. Lett. **87**, 083105 (2005).
[5] N. Zhang, Y. H. Zhang, and Y. J. Xu, Nanoscale **4**, 5792–5813 (2012).
[6] L. Wang, Z. Y. Nie, C. B. Cao, M. W. Ji, L. Zhou, and X. Feng, J. Mater. Chem. A **3**, 3710–3718 (2015).
[7] Y. Q. Li, Z. Y. Wang, B. B. Huanga, and Y. Dai, Appl. Surf. Sci. **347**, 258–264 (2015).
[8] G. Liu, H. G. Yang, X. W. Wang, L. N. Cheng, J. Pan, G. Q. Lu, and H.-M. Cheng, J. Am. Chem. Soc. **131**(36), 12868–12869 (2009).
[9] H. J. Dong, J. X. Sun, G. Chen, C. M. Li, Y. D. Hu, and C. D. Lv, Phys. Chem. Chem. Phys. **16**, 23915–23921 (2014).

[10] Z. G. Yi, J. H. Ye, N. Kikugawa, T. Kako, S. X. Ouyang, H. Stuart-Williams, H. Yang, J. Y. Cao, W. J. Luo, Z. S. Li, Y. Liu, and R. L. Withers, Nat. Mater. **9**, 559–563 (2010).
[11] R. Konta, H. Kato, H. Kobayashi, and A. Kudo, Phys. Chem. Chem. Phys. **5**, 3061–3065 (2003).
[12] J. G. Yu, G. P. Dai, and B. B. Huang, J. Phys. Chem. C **113**(37), 16394–16401 (2009).
[13] S. X. Ouyang, Z. S. Li, Z. Ouyang, T. Yu, J. H. Ye, and Z. G. Zou, J. Phys. Chem. C **112**(8), 3134–3141 (2008).
[14] H. J. Dong, G. Chen, J. X. Sun, C. M. Li, Y. G. Yu, and D. H. Chen, Appl. Catal., B **134–135**, 46–54 (2013).
[15] P. Wang, B. B. Huang, X. Y. Qin, Y. Dai, J. Y. Wei, and M.-H. Whangbo, Angew. Chem., Int. Ed. **47**, 7931–7933 (2008).
[16] P. Wang, B. B. Huang, X. Y. Zhang, H. Jin, Y. Dai, Z. Y. Wang *et al.*, Chem.–Eur. J. **15**, 1821–1824 (2009).
[17] Z. F. Zheng, C. Chen, A. Bo, F. S. Zavahir, E. R. Waclawik, J. Zhao, D. J. Yang, and H. Y. Zhu, ChemCatChem **6**, 1210–1214 (2014).
[18] Y. P. Bi, S. X. Ouyang, N. Umezawa, J. Y. Cao, and J. H. Ye, J. Am. Chem. Soc. **133**, 6490–6492 (2011).
[19] G. P. Dai, J. G. Yu, and G. Liu, J. Phys. Chem. C **116**, 15519–15524 (2012).
[20] J. T. Tang, Y. H. Liu, H. Z. Li, Z. Tan, and D. T. Li, Chem. Commun. **49**, 5498–5500 (2013).
[21] W. J. Wang, B. B. Huang, X. C. Ma, Z. Y. Wang, Y. Dai, M. H. Whangbo *et al.*, Chem.–Eur. J. **19**, 14777 (2013).
[22] R. Zhang, Y. Dai, Z. Z. Lou, Z. J. Li, b. Z. Y. Wang, X. Y. Qin, and B. B. Huang, CrystEngComm **14**(16), 4931–4934 (2014).
[23] Z. Z. Lou, B. B. Huang, Z. Y. Wang, X. C. Ma, X. Y. Zhang, Y. Dai, M. H. Whangbo *et al.*, Chem. Mater. **26**, 3873–3875 (2014).
[24] T.-G. Kim, D.-H. Yeon, T. Kim, J. Lee, and S.-J. Im, Appl. Phys. Lett. **103**, 043904 (2013).
[25] See supplementary material at http://dx.doi.org/10.1063/1.4928595 for more details of experiment and calculation results.